Eur. Phys. J. B **9**, 315–321 (1999)

THE EUROPEAN PHYSICAL JOURNAL B

EDP Sciences
© Società Italiana di Fisica
Springer-Verlag 1999

Oxidation of GaN{0001}-1×1 surfaces at room temperature

O. Janzen[a], Ch. Hahn, and W. Mönch

Laboratorium für Festkörperphysik, Gerhard-Mercator-Universität Duisburg, 47048 Duisburg, Germany

Received 4 September 1998 and Received in final form 6 November 1998

Abstract. The interaction of unexcited oxygen molecules with clean GaN{0001}-1×1 surfaces was investigated using X-ray photoemission spectroscopy (XPS), Auger electron spectroscopy (AES), and low-energy electron diffraction (LEED). Clean surfaces were prepared by a HF dip followed either by desorption of Ga films deposited at room temperature or by nitrogen-ion bombardment and annealing. During exposures in the range from 0.3 up to 10^{15} L-O_2 any excitations of the oxygen were avoided. Oxygen coverages determined from the XPS and the AES data differ by a factor of two. The larger XPS-derived coverages are considered to be more reliable since the AES signals decayed during data recording. The oxygen uptake takes place in two consecutive stages. The first one is identified as dissociative chemisorption and the second one is tentatively attributed to field-assisted diffusion by the Mott-Cabrera mechanism. The dissociative chemisorption is characterized by an initial sticking coefficient of 0.12 ± 0.08 and a saturation coverage of 0.79 ± 0.1 monolayers that is reached after exposures of 10^3 L-O_2. The second mechanism sets in at exposures to 10^8 L-O_2 but reaches no saturation even with the largest doses applied.

PACS. 81.65.Mq Oxidation – 81.05.Ea III-V semiconductors – 82.65.My Chemisorption

1 Introduction

Gallium nitride is a compound semiconductor with a wide direct band gap. As well as other III-nitrides it has attracted great interest because of its applications in optoelectronic devices. Besides light-emitting diodes and blue lasers that already reached the market, III-nitrides are also suitable materials for photocathodes and cold-cathode emission devices [1–3]. A prerequisite for efficient electron emission is that the vacuum level is moved to below the conduction-band bottom in the bulk. Such behavior is called effective negative electron affinity (NEA). Recently, Eyckeler *et al.* [4] found that already a third of a monolayer of cesium adsorbed on *p*-GaN{0001} surfaces suffices to produce effective NEA.

Surface preparation and structure generally influence and sometimes even determine the properties of semiconductor devices. Oxidation studies at room temperature are of special importance also with regard to surface passivation. To the best of our knowledge, Bermudez [5] published the only experimental study that addressed the interaction of oxygen with clean GaN surfaces at room temperature. He found the oxygen uptake to saturate after exposures of only 200 L-O_2 but he did not apply more than 3 000 L-O_2. Exposures are generally given in Langmuirs (L) where 1 L is defined as 10^{-6} torr s $= 1.33 \times 10^{-4}$ Pa s and corresponds to 3.6×10^{14} O_2 molecules impinging per cm^2 at room temperature. To monitor the oxygen pressure during exposures, Bermudez used a hot-filament ionization gauge. However, such pressure gauges are known to stimulate the oxygen uptake on semiconductor surfaces [6,7]. Such, as it is called, *excited oxygen* may be avoided using, for example, gas-friction and thermal-conductance gauges [8].

In this investigation we studied the oxygen uptake of clean GaN{0001}-1×1 surfaces at room temperature during exposures ranging up to 10^{15} L of unexcited oxygen molecules. We used both electron-excited Auger electron spectroscopy (e-AES) and X-ray photoemission spectroscopy (XPS) to monitor the oxygen uptake. This enables us to compare directly data obtained by AES and XPS. Another reason for using both spectroscopies is that we found the O(*KLL*) AES signal to reduce with increasing time of exposure to the primary electron beam.

2 Experimental

The experiments were performed in a stainless-steel ultrahigh vacuum (UHV) system consisting of a rapid load-lock, a preparation chamber, and an analysis chamber. Gate valves separated the three chambers and the samples were transferred between them by means of magnetically coupled rods. Both the analysis and the preparation chamber had base pressures of approximately 2×10^{-8} Pa. The load-lock was evacuated by a turbomolecular pump and reached a pressure below 10^{-4} Pa within 10 minutes. The analysis chamber was equipped with a four-grid optic (Varian) for low-energy electron diffraction (LEED) and a cylindrical mirror analyzer (CMA, Varian) with an

[a] e-mail: oliver_janzen@uni-duisburg.de

integral electron-gun for AES as well as an X-ray source with a Mg/Zr double anode and a concentric hemispherical analyzer (VSW) for XPS. The photoemitted electrons were detected at normal emission. For *in-situ* cleaning the preparation chamber contained a Knudsen-cell for gallium evaporation and an ion gun for nitrogen sputtering.

The method of oxygen exposure varied depending on the exposure range. Low doses up to 3×10^4 L-O_2 were applied in the preparation chamber with a gas doser where the samples were placed at a distance of 5 mm in front of the glass capillary array used for beam shaping. For doses in the range from 10^5 up to 3×10^9 L-O_2, the preparation chamber was backfilled to constant O_2 pressures ranging from 10^{-2} to 250 Pa for time intervals varying from 200 up to 1000 s. In the same way but in the load-lock, doses up to 10^{13} L-O_2 were applied. Even larger exposures were achieved by storing the samples in a separate container at 1 bar of pure O_2 for up to two weeks. During the transfer between the UHV system and the container the samples were exposed to ambient air for a few minutes. To avoid any stimulation of the oxygen uptake, the samples were kept in the dark and the oxygen pressure was monitored by either gas-friction or thermal-conduction gauges only.

The samples used were α-GaN{0001} epilayers grown by metal-organic vapor-phase epitaxy (MOVPE) on sapphire with a thickness of 1.83 μm (Cree Research). Their polarity, *i.e.* (0001) or $(000\overline{1})$, was not specified by the vendor. We applied the following procedures to obtain clean surfaces. All samples were first dipped into hydrofluoric acid for 1 min which was then diluted by a buffered HF solution (HF:NH_4F:NH_4OH) with pH = 9, subsequently rinsed in de-ionized water, blown dry with nitrogen, and immediately transferred into the UHV system. As *in-situ* preparation we employed two procedures. One of them, the Ga-preparation, consists of the deposition of a 10 nm thick Ga film at room temperature and its desorption at approximately 850 °C. The calibration error of the sample temperature amounts to $\pm$20 °C. The other procedure, the N-preparation, was nitrogen-ion bombardment followed by annealing at also approximately 850 °C. Details of this treatment are described in reference [5]. The latter procedure was applied to avoid any possible presence of excess Ga after Ga-preparations that might distort the oxygen uptake. Both preparation methods produce clean and well-ordered GaN{0001}-1×1 surfaces [9].

Mg($K\alpha$)-excited XPS and electron-excited AES were used to check the surface cleanliness and to determine the oxygen uptake. Here, XPS was always performed before AES to exclude any effects of the primary electron beam. AES spectra were recorded as first derivatives and intensities of the lines were taken as the peak-to-peak heights (PPH) of the Auger signals. The GaN{0001} surfaces were considered to be stoichiometric when the ratio of the N(KVV) and Ga(LMM) intensities amounted to 0.79 ± 0.06. This value was already observed after the HF dip. Irrespective of the *in-situ* treatment used, all samples displayed residual C(KLL) and O(KLL) signals that came up to 1% of the intensity of the Ga(LMM) substrate signal at maximum. After oxygen exposures the

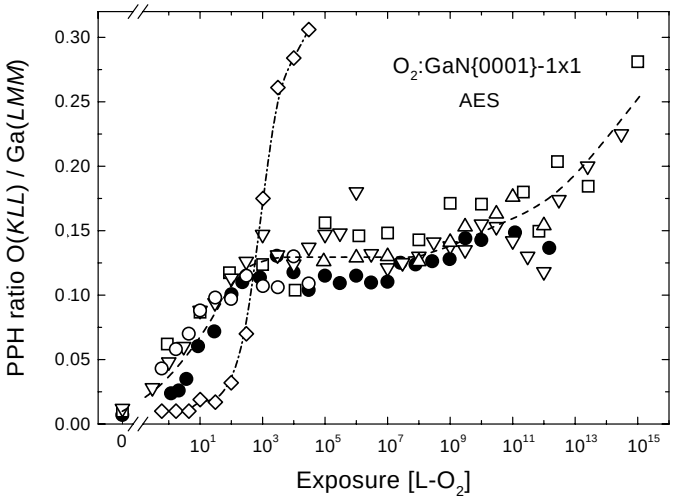

Fig. 1. Peak-to-peak height ratio of O(KLL) and Ga(LMM) AES-signals recorded with differently prepared GaN{0001}-1×1 surfaces as a function of exposure to molecular oxygen at room temperature. Solid and open symbols represent N- and Ga-prepared samples; (◊) data were recorded with a Ga-rich surface. The dashed and dotted lines are meant to guide the eye.

O(KLL) and Ga(LMM) lines were recorded first within two minutes. In a subsequent second run, the Ga(MVV), N(KVV), and C(KLL) signals were taken at the same spot within another 10 minutes. During the latter procedure the O(KLL)/Ga(LMM) intensity ratio decreased by about 10 to 20% compared with the preceding, more rapid measurement. In plotting AES intensity ratios against exposures we will only consider results of the faster first recordings.

The Ga-prepared samples displayed 1×1 LEED patterns. However, the normal spots periodically split into circularly arranged sextets as a function of the primary electron energy, *i.e.*, the multiplet rings periodically first widened, then shrunk, and eventually coalesced. The N-prepared samples showed no LEED patterns immediately after ion-bombardment. After annealing, these surfaces also displayed 1×1 patterns the spots of which again periodically split into ring-shaped sextets with increasing energy of the primary electrons. However, the multiplet spots appeared to be sharper than those observed with the Ga-prepared surfaces. This splitting of the normal-order spots on GaN{0001} surfaces annealed at elevated temperatures has been explained by spiral arrangements of steps. Details of these observations and their analysis are discussed in reference [9].

3 Results

Figure 1 displays PPH-ratios of the O(KLL) and Ga(LMM) signals recorded with differently prepared GaN{0001}-1×1 surfaces as a function of exposure to unexcited molecular oxygen at room temperature. The N(KVV)/Ga(LMM) PPH-ratios were the same after all

oxygen exposures. In Figure 1 open symbols and solid circles stand for stoichiometric Ga- and N-prepared surfaces, respectively. The diamonds show the oxygen uptake of a surface with excess Ga. This latter surface exhibited a N(*KVV*)/Ga(*LMM*) PPH-ratio of 0.58 instead of 0.79 ± 0.06 that characterizes stoichiometric surfaces. The dashed and dotted lines are meant to guide the eyes of the reader only.

At stoichiometric surfaces the oxygen uptake evidently proceeds in two subsequent stages. The first one is effective already at the lowest doses applied, 0.3 L-O_2, and tends to saturate at 10^3 L-O_2. After further exposures, the O(*KLL*)/Ga(*LMM*) intensity ratio remains unchanged until at approximately 10^8 L-O_2 a second stage sets in. The oxygen signal shows no tendency to saturate up to the largest exposures applied. The oxygen uptake apparently develops the same way irrespective of the surface preparation used although it seems to be slightly larger on Ga-prepared than on N-prepared samples. However, this can not be proved reliably due to the scatter of the experimental data points.

The initial Auger intensity ratio of the Ga-rich surface was N(*KVV*)/Ga(*LMM*) = 0.58. We estimate the excess Ga on this surface as approximately one additional monolayer. Since gallium monolayers cover 1×1 structures of both GaN(000$\overline{1}$) as well as GaN(0001) surfaces [10] this Ga-rich surface consists of two terminating monolayers of Ga irrespective of its unknown polarity. The oxidation properties of this Ga double layer drastically differs from what is observed with clean, stoichiometric GaN{0001}-1×1 surfaces. The oxidation is inhibited up to exposures of 100 L-O_2 where the oxygen uptake steeply increases. After 3 000 L-O_2, the O(*KLL*)/Ga(*LMM*) intensity ratio amounts to 0.31. This value exceeds the data obtained with stoichiometric surfaces even after the largest exposures of 10^{15} L-O_2.

Figure 2 displays the intensity ratio of the O(1*s*) and Ga(3*p*) photoemission peaks recorded with a Ga-prepared sample as a function of exposure to unexcited oxygen molecules at room temperature. The N(1*s*)/Ga(3*p*) intensity ratio remained the same after all oxygen exposures. In Figure 2 the dashed line is taken from Figure 1 and represents the e-AES data. It was reduced by a factor of 0.83 to scale with the XPS data. The XPS and the AES data develop in the same way as a function of exposure. Due to the line widths of the exciting Mg($K\alpha$) and Zr($M\zeta$) lines we were unable to resolve any chemically shifted components with the Ga(3*p*), N(1*s*), and O(1*s*) XPS and Ga(3*d*) SXPS peaks.

LEED showed that the 1×1 patterns of the clean surfaces changed only slightly with increasing oxygen exposures. Both the width of the normal-order spots and the intensity of the diffuse background increased with the oxygen uptake. The multiplet spots [9] developed into blurred rings around the positions of the normal-order spots. A 1×1 LEED pattern was still observed even after the highest doses of 10^{15} L-O_2.

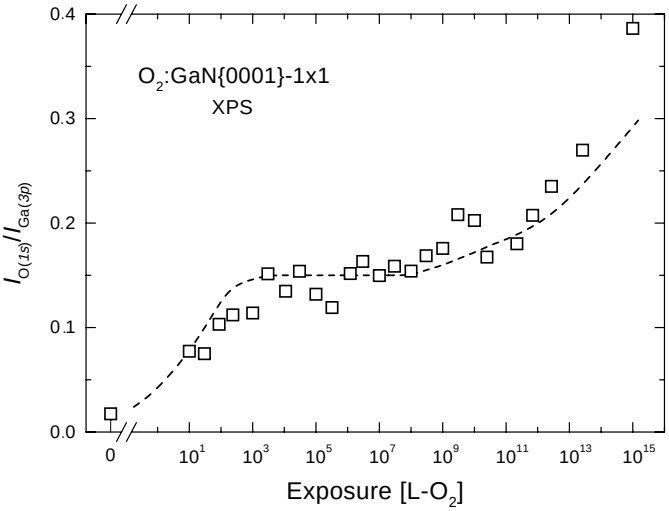

Fig. 2. Intensity ratio of O(1*s*) and Ga(3*p*) XPS-lines recorded with a Ga-prepared GaN{0001}-1×1 surface as a function of exposure to molecular oxygen at room temperature. (□) The data of Figure 1 were recorded simultaneously with the same sample. The dashed line is taken from Figure 1 and scaled to fit the XPS data in the exposure range between 10^3 and 10^7 L-O_2.

4 Discussion

4.1 Quantitative determination of the oxygen uptake

The oxygen uptake of the GaN{0001}-1×1 surfaces will be analyzed by considering the experimental O(*KLL*)/Ga(*LMM*) and O(1*s*)/Ga(3*p*) intensity ratios displayed in Figures 1 and 2, respectively. For submonolayer coverages we will use a simple layer model [11] and assume the adspecies on top of Ga-terminated surfaces. The intensity ratio I_O/I_{Ga} of the oxygen and gallium signals is related to the oxygen coverage as

$$\Theta = \{[1-\exp(-d_{ox}\xi_{Ga})] + (I_{Ga}\sigma_O/I_O\sigma_{Ga}) \times [1-\exp(-d_{0001}\xi_{Ga})]\exp(-d^*_{0001}\xi_{Ga})\}^{-1}. \quad (1)$$

Coverages are measured in monolayers (ML) and we define a monolayer as the density of sites in a bulk GaN(0001) layer, *i.e.*, 1 ML = 1.1×10^{15} cm^{-2}. The distances between and within GaN(0001) bilayers measure $d_{0001} = 0.259$ nm and $d^*_{0001} = 0.064$ nm, respectively. The Ga-O bond length d_{ox} is taken as the sum of the respective covalent radii, 0.199 nm [12]. The inverse of the effective escape depth of the Ga-signal is given by

$$\xi_{Ga} = 1/\lambda_p + 1/\lambda_{Ga}\cos\vartheta, \quad (2)$$

with the attenuation length λ_p of the exciting radiation and the escape length λ_{Ga} and the detection angle ϑ of the Ga signals. AES and XPS differ in that the penetration depth of the of X-rays is much larger than the escape depth $\lambda_{Ga(3p)} = 2.5$ nm of the Ga(3*p*) photoelectrons while in AES the attenuation length $\lambda_p = 4.1$ nm of the 3 keV primary electrons is only larger by a factor of two than the escape length $\lambda_{Ga(LMM)} = 2.4$ nm of the Ga(*LMM*) Auger

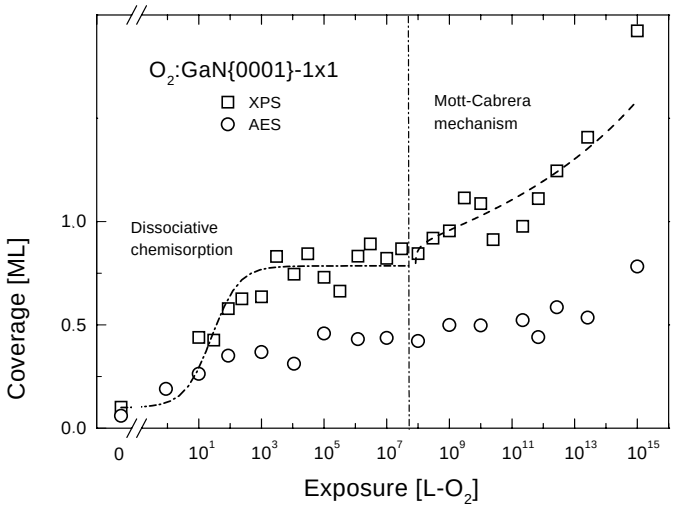

Fig. 3. Oxygen coverages on GaN{0001}-1×1 surfaces as a function of oxygen exposure at room temperature as determined from the XPS data displayed in Figure 2 and the AES data of the same sample shown in Figure 1. The dotted and dashed lines are least-squares fits of equations (5, 6) to the data, respectively.

electrons. Furthermore, the photoelectrons are detected at normal emission while the CMA used in AES has a detection angle $\vartheta_{\mathrm{CMA}} \approx 42°$.

The effective excitation cross-sections σ_{Ga} and σ_{O} of the Ga and the O signals, respectively, were calibrated using polycrystalline Ga_2O_3. Such a layer was grown by exposing a GaN sample to 1 bar of pure O_2 at 900 °C for 7 hours [13]. Scanning transmission electron microscopy gave an oxide thickness of approximately 500 nm. AES and XPS spectra of this sample revealed no nitrogen signal at all and gave the intensity ratios $I_{\mathrm{O}(KLL)}/I_{\mathrm{Ga}(LMM)} = 1.96 \pm 0.01$ and $I_{\mathrm{O}(1s)}/I_{\mathrm{Ga}(3p)} = 2.0 \pm 0.03$, respectively. Since the Ga_2O_3 layer was polycrystalline we used a homogeneous instead of a layer model for the data analysis [11]. We estimate the attenuation lengths $\lambda_{\mathrm{O}(KLL)} = 1.7$ nm, $\lambda_{\mathrm{Ga}(LMM)} = 2.4$ nm, $\lambda_{\mathrm{p}} = 4.1$ nm, $\lambda_{\mathrm{O}(1s)} = 2$ nm, and $\lambda_{\mathrm{Ga}(3p)} = 2.5$ nm [14]. From the experimental intensity ratios $I_{\mathrm{O}(KLL)}/I_{\mathrm{Ga}(LMM)}$ and $I_{\mathrm{O}(1s)}/I_{\mathrm{Ga}(3p)}$ we obtained the ratios of the effective excitation cross-sections $\sigma_{\mathrm{Ga}(LMM)}/\sigma_{\mathrm{O}(KLL)} = 1.68 \pm 0.08$ and $\sigma_{\mathrm{O}(1s)}/\sigma_{\mathrm{Ga}(3p)} = 1.67 \pm 0.08$, respectively.

The numerical evaluation of equation (1) finally gives the oxygen coverage on GaN{0001}-1×1 surfaces as

$$\Theta_{\mathrm{AES}} = (0.148 + 0.318\ I_{\mathrm{Ga}(LMM)}/I_{\mathrm{O}(KLL)})^{-1} \quad (3)$$

for AES and

$$\Theta_{\mathrm{XPS}} = (0.08 + 0.17 I_{\mathrm{Ga}(3p)}/I_{\mathrm{O}(1s)})^{-1} \quad (4)$$

for XPS. Figure 3 displays the oxygen uptake calculated using the AES data shown in Figure 1 and equation (3) and the XPS data plotted in Figure 2 and equation (4). The layer model used is valid for coverages up to one monolayer only and coverages well in excess of this limit have to be described as oxide films. As the data plotted in Figure 3 show, the layer model gives nominal oxygen uptakes that do not exceed two monolayers at maximum. Therefore, we consider nominal oxygen coverages in the range between one and two monolayers as realistic estimates.

The XPS intensity ratios give oxygen coverages that are by a factor of approximately two larger than what is obtained from the AES data. In the range from 10^3 up to 10^7 L-O_2, intermediate saturation coverages of 0.39 ± 0.1 ML and 0.79 ± 0.1 ML are obtained from AES and XPS, respectively. Similar observations have been reported for the oxygen uptake on cleaved GaAs(110) surfaces at room temperature. In their investigations, Bartels and Mönch [15] and Hughes and Ludeke [16] used AES and XPS, respectively. As in the present experiments with GaN, the AES and XPS signals recorded with cleaved GaAs surfaces developed in the same way as a function of oxygen exposure and the XPS-derived coverages exceeded those obtained from the AES data by a factor of two.

The difference between the AES- and XPS-derived coverages might be a result of the assumptions of the layer model used or of experimental details that are not properly considered. Since the attenuation length of 3 keV electrons is much smaller than the penetration depth of Mg($K\alpha$) radiation AES is more surface-sensitive than XPS. Therefore, the data analysis would give lower AES- than XPS-derived oxygen coverages if oxygen diffuses into the substrate rather than adsorbs on the surface as assumed in the layer model. However, the escape lengths of the Auger and the photoemitted electrons are almost equal and, therefore, in-diffusion of oxygen during exposures may be ruled out as an explanation of the larger XPS-derived oxygen coverages. We also calibrated the ratios of the effective cross-section for AES and XPS with one and the same Ga_2O_3 sample. Thus, mechanisms that change the oxygen surface coverage during measurements might be responsible for the differences in AES- and XPS-derived coverages. In AES, the beam of the primary 3 keV electrons was set to a current of 2 μA and focused to a spot of approximately 40 μm in diameter. As already mentioned in Section 3, prolonged exposures of oxygen-covered GaN surfaces to the e-beam reduced the O(KLL) line. This may be due to oxygen desorption or intermixing caused by local heating by the electron beam. Although the AES signals considered for determining the oxygen uptake were taken within two minutes a loss of oxygen by whatever mechanism can not be excluded during this initial interval of time. Therefore, we consider the XPS data and, consequently, the XPS-derived oxygen coverages to stand for the undistorted oxygen uptake on GaN{0001}-1×1 surfaces.

4.2 Oxidation mechanisms

4.2.1 Dissociative chemisorption

The oxygen uptake at room temperature proceeds not only on GaN{0001}-1×1 surfaces in two well-separated

stages but the same has been reported for Si(111)-2×1 [17], Si(111)-7×7 [17], Si(001)-2×1 [18], and 3C-SiC(001)-2×1 surfaces [19]. Dissociative chemisorption and field-assisted oxidation by the Mott-Cabrera mechanism were identified as the underlying mechanisms in the regimes of small and higher exposures, respectively. At cleaved GaAs(110) surfaces [20] both processes directly merge since the initial sticking coefficient of dissociative chemisorption is very small. As with the other semiconductors, we attribute the two subsequent oxidation stages observed with GaN{0001}-1×1 surfaces at room temperature to dissociative chemisorption and field-assisted oxidation.

For dissociative chemisorption the coverage Θ as a function of the total number N of molecules impinging per unit area is given by [21]

$$\Theta = S_0\Theta_s N/(\sigma_{sub} + S_0 N), \tag{5}$$

where S_0 and Θ_s are the initial sticking coefficient and the saturation coverage, respectively. The total number σ_{sub} of surface sites per unit area amounts to 1.1×10^{15} cm^{-2} in GaN{0001} planes. The dash-dotted line in Figure 3 is a least-squares fit of equation (5) to the XPS data. The two fitting parameters, initial sticking coefficient and saturation coverage, resulted as $S_0 = 0.12 \pm 0.08$ and $\Theta_s = 0.79 \pm 0.1$ ML.

The sticking probability of oxygen at room temperature is by some orders of magnitude larger on GaN{0001} surfaces than on other III-V compound semiconductors. Dissociative chemisorption sets in at exposures larger than 10^3 L-O_2 on, for example, cleaved GaAs-, GaSb-, InP-, and InAs(110) surfaces [22,23] as well as on GaAs(001)-4×1 and GaAs(311)-1×1 surfaces [8]. Similar differences were also observed with, on the one hand, Si(111)-7×7 [24,25] and, on the other hand, Si(111)-2×1 [6,26] surfaces. The surfaces mentioned differ not only in their oxidation behavior but also in their electronic surface properties. Cleaved Si(111) and III-V(110) as well as GaAs(001) surfaces have in common that the occupied and empty bands of their dangling-bonds are separated by an energy gap (see, for example, Ref. [27]). Their surface band structures are said to be semiconducting. On the other hand, a feature of the dangling bonds of Si(111)-7×7 (see, for example, Ref. [27]) and GaN{0001}-1×1 surfaces [28] is that their character is metallic. It is this difference in the dangling bonds that might account for the drastically larger reactivities of Si(111)-7×7 and GaN{0001}-1×1 surfaces in comparison with Si(111)-2×1, III-V(110)-1×1, and GaAs(001)-4×1 surfaces.

Elsner *et al.* [29] theoretically investigated oxygen chemisorption on GaN(000$\overline{1}$)- as well as GaN(0001)-1×1 surfaces using a charge selfconsistent density-functional based tight-binding approach. They assumed both kinds of surfaces to be covered by Ga layers and found the oxygen uptake to saturate at approximately 0.75 to 1 ML. Their findings agree with our experimental results.

4.2.2 Mott-Cabrera mechanism

Oxide films are not expected to grow at room temperature since the diffusion coefficients are by far too small. The Mott-Cabrera mechanism [30,31] explains the growth of oxide layers taking place at room temperature by field-assisted diffusion of ionic species. The respective electric field across the oxide films is attributed to the presence of oxygen ions on the film surface. They take up electrons *via* tunneling from the semiconductor substrates [22]. The Mott-Cabrera mechanism describes the oxide film growth by an inverse-logarithmic law, *i.e.*,

$$\frac{1}{\Theta} = \frac{1}{\Theta_c} - \frac{1}{\Theta_M}\ln[(N - N_c)/a + 1], \tag{6}$$

where the parameters N_c and Θ_c are the oxygen exposure and coverage at the onset of the Mott-Cabrera mechanism, $\Theta_M = e_0 V_M/k_B T$ is the reduced Mott potential V_M, and a describes the slope of the initial oxidation rate. Here, k_B and T are Boltzmann's constant and the temperature, respectively.

Although the estimated nominal oxygen uptake in the second stage that follows dissociative chemisorption does not exceed the equivalent of two monolayers we tentatively fitted equation (6) to the experimental XPS data displayed in Figure 3. The least-squares fit shown gave $N_c = 8.3\times10^7$ L-O_2, $\Theta_c = 0.79$ ML, $V_M = 0.87$ V, and $a = 5.3\times10^5$ L. These fitting parameters are in the range of what has been reported for other semiconductors. Even though the fit appears to be good more experiments are certainly needed to ascertain that the Mott-Cabrera mechanism governs the second stage of oxygen uptake at GaN{0001}-1×1 surfaces at room temperature.

4.2.3 Unexcited versus excited oxygen

The only other investigation on the chemisorption of oxygen on GaN{0001}-1×1 surfaces at room temperature has been published by Bermudez [5]. However, there is one essential difference between his and our studies. Bermudez used an ionization gauge for monitoring the oxygen pressure during exposures. He was well aware of the early observation of Archer and Gobeli's [6] that the use of hot-filament ionization devices during oxygen exposures dramatically stimulates the oxygen uptake on cleaved Si(111)-2×1 surfaces. Kraus *et al.* [8] demonstrated that even cold-cathode ionization gauges enhance the oxygen uptake on GaAs(001)-4×1 surfaces. In the present investigation, on the other hand, we avoided any such possible stimulation by using gas-friction and thermal-conductance gauges only [8]. Nevertheless, Figure 4 displays Bermudez's AES data together with ours that were already shown in Figure 1. Surprisingly, both sets of experimental data almost perfectly agree, *i.e.*, there is no difference in whether the GaN{0001} surfaces were exposed to excited, as it is called, or unexcited oxygen. As we did in Section 4.1 Bermudez also analyzed his AES data using a layer model and he obtained a saturation coverage of 0.4 ML.

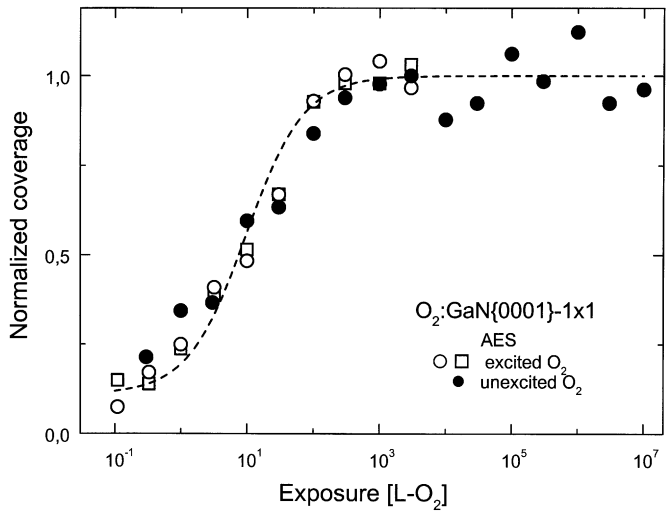

Fig. 4. Normalized AES coverages on GaN{0001}-1×1 surfaces as a function of exposure to unexcited and excited oxygen. The clean surfaces were N-prepared. (•) Data for unexcited O_2 from Figure 1; (□, ○) data for excited O_2 from reference [5]. The dashed line is taken from Figure 3.

This value agrees with the saturation coverage of 0.39 ML that we derived from our AES results. This is not surprising since the settings of the electron gun were similar in the both studies. Nevertheless, we rely on the by a factor of two larger oxygen coverages that we obtained from the XPS data for the reasons discussed in Section 4.1.

The observation that there is no difference in the dissociative chemisorption of oxygen on whether GaN{0001} surfaces are exposed to excited or unexcited oxygen may have a simple explanation. The main difference in the oxidation behavior of GaN{0001} and, for example, cleaved GaAs(110) surfaces is that GaN takes up oxygen already after the lowest dose of 0.3 L-O_2 applied whereas GaAs(110) surfaces are inert up to 10^5 L-O_2. This means that the initial sticking coefficients differ by a factor of approximately 10^5. The use of "excited" oxygen increases the initial sticking coefficient of oxygen on GaAs(110) surfaces by up to a factor of 500 [7] but even then it remains much smaller than what is observed with GaN{0001} surfaces.

5 Summary and conclusions

The present investigation on the interaction of GaN{0001}-1×1 surfaces with unexcited molecular oxygen at room temperature revealed two subsequent reaction mechanisms. The kinetics of the oxygen uptake was found to be the same irrespective of whether we applied the Ga- or the N-preparation to obtain clean GaN{0001}-1×1 surfaces. However, the presence of an additional monolayer of gallium drastically reduces the initial sticking coefficient by a factor of approximately 100. "Excited" oxygen, on the other hand, produced by ionization gauges used for monitoring the oxygen supply was found to have the same reaction kinetics as unexcited molecular oxygen.

The first of the two reaction mechanisms was identified as dissociative chemisorption. As on Si(111)-7×7 surfaces, the initial sticking coefficient is very large in comparison with what is observed with cleaved surfaces of silicon as well as III-V compound semiconductors. This behavior seems to correlate with the character of the dangling-bond band structure that is metallic on the highly reactive Si(111)-7×7 and GaN{0001}-1×1 surfaces but semiconducting on the cleaved Si(111)-2×1 and III-V(110) surfaces of low reactivity. The dissociative chemisorption on GaN{0001}-1×1 surfaces saturates at an oxygen coverage of 0.79 ML. The second reaction path that sets in at exposures larger than 10^8 L-O_2 is tentatively attributed to field-assisted diffusion by the Mott-Cabrera mechanism. This assignment, as plausible it is, requires additional investigations. Even after the largest exposures applied, the nominal oxygen uptake of GaN{0001}-1×1 surfaces at room temperature does not exceed two monolayers at maximum which are hard to describe as an oxide film.

The authors like to thank H. Lakner and G. Brockt, Department of Electrical Engineering of the Gerhard-Mercator-Universität Duisburg, for the scanning transmission electron microscopy with the thermally oxidized GaN sample. J. Elsner is gratefully acknowledged for fruitful discussions and for providing preprints of unpublished work. This investigation was partially supported by grant Mo318/28-1 of the Deutsche Forschungsgemeinschaft.

References

1. A.T. Sowers, J.A. Christman, M.D. Bremser, B.L. Ward, R.F. Davis, R.J. Nemanich, Appl. Phys. Lett. **71**, 2289 (1997).
2. B.V. Spitsyn, V.V. Zhirnov, A.N. Blaut-Bachev, L.V. Bormatova, A.F. Belyanin, P.V. Pashchenko, L.I. Bouilov, E.I. Givargizov, Diamond. Relat. Mater. **7**, 692 (1998).
3. R.D. Underwood, S. Keller, U.K. Mishra, D. Kapolnek, B.P. Keller, S.P. DenBaars, J. Vac. Sci. Technol. B **16**, 822 (1998).
4. M. Eyckeler, W. Mönch, T.U. Kampen, R. Dimitrov, O. Ambacher, M. Stutzman, J. Vac. Sci. Technol. B **16**, 2224 (1998).
5. V.M. Bermudez, J. Appl. Phys. **80**, 1190 (1996).
6. R.J. Archer, G.W. Gobeli, J. Phys. Chem. Solids **26**, 343 (1965).
7. P. Pianetta, I. Lindau, C.M. Garner, W.E. Spicer, Phys. Rev. B **18**, 2792 (1978).
8. P. Kraus, W. Nunes Rodrigues, W. Mönch, Surf. Sci. **219**, 107 (1989).
9. O. Janzen, Ch. Hahn, W. Mönch, Eur. Phys. J. B **7**, 1 (1999).
10. A.R. Smith, R.M. Feenstra, D.W. Greve, J. Neugebauer, J.E. Northrup, Phys. Rev. Lett. **79**, 3934 (1997).
11. R. Memeo, F. Ciccacci, C. Mariani, S. Ossicini, Thin Solid Films **109**, 159 (1983).
12. *Table of Periodic Properties of the Elements* (Sargent-Welch, Skokie, IL, 1980).

13. S.D. Wolter, B.P. Luther, D.L. Waltemeyer, C. Önneby, S.E. Mohney, R.J. Molnar, Appl. Phys. Lett. **70**, 2156 (1997).
14. M.P. Seah, W.A. Dench, Surf. Interf. Anal. **1**, 2 (1979).
15. F. Bartels, W. Mönch, Surf. Sci. **143**, 315 (1984).
16. G. Hughes, R. Ludeke, J. Vac. Sci. Technol. B **4**, 1109 (1986).
17. A. Stockhausen, T.U. Kampen, W. Mönch, Appl. Surf. Sci. **56-58**, 795 (1992).
18. J. Westermann, H. Nienhaus, W. Mönch, Surf. Sci. **311**, 101 (1994).
19. V. van Elsbergen, O. Janzen, W. Mönch, Mat. Sci. Eng. B **46**, 366 (1997).
20. W. Mönch, Surf. Sci. **168**, 577 (1986).
21. W.H. Weinberg, in *Kinetics of Interface Reactions*, edited by M. Grunze, H.J. Kreuzer (Springer, Berlin, 1986), p. 94.
22. F. Bartels, W. Mönch, Vacuum **41**, 667 (1990).
23. H.U. Baier, L. Koenders, W. Mönch, Surf. Sci. **184**, 345 (1987).
24. C.A. Carocella, J. Comas, Surf. Sci. **15**, 303 (1969).
25. P. Gupta, C.H. Mak, P.A. Coon, S.M. George, Phys. Rev. B **40**, 7739 (1989).
26. H. Ibach, K. Horn, R. Dorn, H. Lüth, Surf. Sci. **38**, 433 (1973).
27. W. Mönch, *Semiconductor Surfaces and Interfaces*, 2nd edn. (Springer, Berlin, 1995).
28. A.R. Smith, R.M. Feenstra, D.W. Greve, M.-S. Shin, M. Skowronski, J. Neugebauer, J.E. Northrup, J. Vac. Sci. Technol. B **16**, 2242 (1998).
29. J. Elsner, R. Gutierrez, B. Hourahine, R. Jones, M. Haugk, Th. Frauenheim, Solid State Commun. **108**, 953 (1998).
30. N.F. Mott, Trans. Faraday Soc. **43**, 429 (1947).
31. N. Cabrera, N.F. Mott, Rep. Prog. Phys. **12**, 163 (1949).